Interpreting the CMS $\ell^+\ell^-jj+$ missing transverse energy excess with a leptoquark model

Ben Allanach,[1] Alexandre Alves,[2,*] Farinaldo S. Queiroz,[3,4] Kuver Sinha,[5] and Alessandro Strumia[6,7]

[1]*DAMTP, CMS, Wilberforce Road, University of Cambridge, Cambridge CB3 0WA, United Kingdom*
[2]*Departamento de Ciências Exatas e da Terra, Universidade Federal de São Paulo,*
Diadema-SP 09972-270, Brazil
[3]*Department of Physics and Santa Cruz Institute for Particle Physics, University of California,*
Santa Cruz, California 95064, USA
[4]*International Institute of Physics, UFRN, Avenida Odilon Gomes de Lima 1722,*
Capim Macio, 59078-400 Natal-RN, Brazil
[5]*Department of Physics, Syracuse University, Syracuse, New York 13244, USA*
[6]*Dipartimento di Fisica dell' Universita di Pisa and INFN, Pisa, 56126 Italy*
[7]*National Institute of Chemical Physics and Biophysics, 12618 Tallinn, Estonia*

We present a model of leptoquarks (LQs) with a significant partial branching ratio into an extra sector, taken to be a viable dark matter candidate, other than the canonical lepton and jets final state. For LQs with mass around 500 GeV, the model reproduces the recent excess claimed by the CMS Collaboration in the $\ell^+\ell^-jj\not{E}_{\mathrm{T}}$ final state: the event rate, the distribution in the dilepton invariant mass and the rapidity range are compatible with the data. The model is compatible with other collider bounds including LQ searches, as well as bounds from meson mixing and decays. Prospects of discovery at run II of the LHC are discussed.

PACS numbers: 14.80.Sv, 12.60.Cn, 12.60.Fr, 13.85.Rm

I. INTRODUCTION

The CMS Collaboration reported a 2.6σ excess compared with Standard Model expectations in $\ell^+\ell^-jj\not{E}_{\mathrm{T}}$ events, containing two opposite-sign same-flavor leptons $\ell^\pm = \{e^\pm, \mu^\pm\}$, at least two jets and missing transverse momentum $\not{E}_{\mathrm{T}}$ [1] with 19.4 fb^{-1} of integrated luminosity at a center of mass energy of 8 TeV. The excess was found in the central region with lepton pseudorapidities $|\eta_\ell| \leq 1.4$, after event selection and flavor subtraction cuts, and with dilepton invariant mass $m_{\ell\ell} < 80$ GeV, as shown in Fig. 1. No excess is seen in other regions nor in the trilepton channel.

The excesses were found in the context of searches for edges in $m_{\ell\ell}$. The triangular edge is a classic supersymmetry signal. Interpretations of the CMS excess in the context of the so-called golden cascade $(\tilde{\chi}_2^0 \rightarrow \tilde{\ell}^\pm \ell^\mp \rightarrow \tilde{\chi}_1^0 \ell^\pm \ell^\mp)$ have been proposed $(\tilde{\chi}_1^0, \tilde{\chi}_2^0$ and $\tilde{\ell}$ are the lightest neutralino, the next-to-lightest neutralino and the slepton, respectively). Since direct electroweak production of $\tilde{\chi}_2^0$ has a too small cross section to provide a large enough rate while evading previous collider bounds from LEP, assistance from colored particle production is required. The decay chain could start with $\tilde{t} \rightarrow t\tilde{\chi}_2^0$ [2] or $\tilde{q} \rightarrow q\tilde{\chi}_2^0$ [3]. The former interpretation is constrained by the fact that the CMS study did not observe a large excess in trilepton final states, which should be present from the leptonic top quark decay. The CMS study itself opted for an

explanation in terms of light sbottoms $\tilde{b} \rightarrow b\tilde{\chi}_2^0$ and $\tilde{\chi}_2^0 \rightarrow \tilde{\chi}_1^0 \ell^+\ell^-$, although no b-jet requirement was made on the final states. Reference [4] explored the parameter space in order to simultaneously satisfy bounds from four charged lepton production. Recently, however, several potential supersymmetry (SUSY) scenarios explaining the CMS excess have been shown to be in tension with existing experimental data [5].
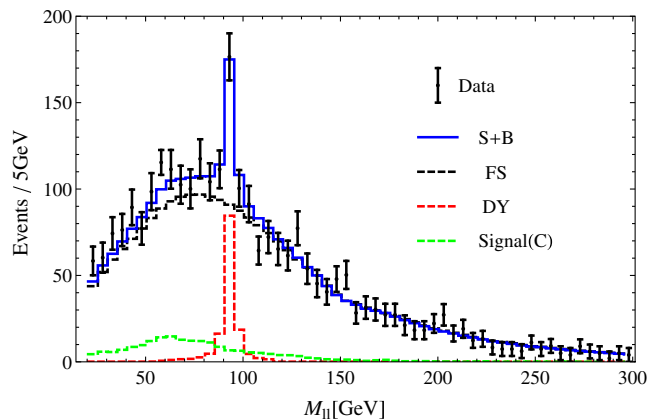

FIG. 1 (color online). Dilepton invariant mass spectrum of CMS $\ell^+\ell^-jj\not{E}_{\mathrm{T}}$ events: expected non-DY background (black histogram), expected DY (red histogram), expected signal for benchmark C (green histogram) and expected signal plus background for benchmark C (blue histogram). Twenty-one signal events are expected for $m_{\ell\ell} > 100$ GeV, which is compatible with the CMS data.

*aalves@unifesp.br

The purpose of this paper is to point out that the CMS excess can be explained by a different, nonsupersymmetric class of models with leptoquarks (LQs) [6–12]. In a model of LQs presented in [13] by some of the authors, the LQ had branchings to three possible final states: (i) the usual final state with charged lepton and jet; (ii) final state with jets and missing energy E_T in the form of dark matter (DM); and (iii) final state with charged lepton, jets and E_T in the form of DM. By a combination of branchings and kinematics, the model was able to account for the mild excess in the $eejj$ and $e\nu jj$ channels observed by a recent CMS search [14,15] for first generation LQs in the mass range 550–650 GeV. To account for the event rate observed by CMS in these first generation LQ searches, the branching ratio of the LQ into electrons and quarks was taken to be $\approx 15\%$. A viable DM sector was constructed which accounted for the remaining branching ratio through channels (ii) and (iii) mentioned above.

In this work, we note that the same framework, through its connection to DM, interestingly enables us to fit the CMS $\ell^+\ell^- jjE_T$ excess. Figure 1 exemplifies how the $\ell^+\ell^- jjE_T$ excess can be reproduced by LQs with ≈ 500 GeV masses: the model predicts a peak in $m_{\ell\ell}$, which fits data roughly as well as the triangular edge searched for by CMS. The model also predicts small numbers of events in the forward region and for trilepton final states, also compatible with the CMS measurements. The model is compatible with flavor constraints, as well as constraints from other LHC searches. We will see that the benchmark point that best fits the CMS $\ell^+\ell^- jjE_T$ excess is around ~ 500 GeV where there is no excess in the $eejj$ and $e\nu jj$ channels. This necessitates a different choice of branchings and benchmark from [13].

II. THE MODEL

We consider LQs that do not lead to proton decay at a renormalizable level: either a scalar R_2 in the $(3, 2, 7/6)$ representation of $SU(3) \otimes SU(2) \otimes U(1)$ that can couple to $\bar{Q}e$ and to $L\bar{u}$; or a scalar $\tilde{R}_2$ in the $(3, 2, 1/6)$ representation (the same as the quark doublet Q) that can couple to $L\bar{d}$ [16,17]. We note that dimension-five operators involving these LQs can lead to proton decay; these have to be forbidden by a discrete symmetry, as shown in detail in [13].

We focus on $\tilde{R}_2$ because its quantum numbers are favorable from a DM perspective, as we will clarify later. Pair production of $\tilde{R}_2$ via gluon fusion and quark-antiquark annihilation thus constitutes our main example. Its Lagrangian couplings are

$$-\lambda_d^{ij} \bar{d}_R^i \tilde{R}_2^T \epsilon L_L^j + \text{H.c.}, \tag{1}$$

where i, j denote flavor indices. In the above,

$$\tilde{R}_2 = \begin{pmatrix} V_\alpha \\ Y_\alpha \end{pmatrix}, \qquad \epsilon = \begin{pmatrix} 0 & 1 \\ -1 & 0 \end{pmatrix}, \qquad L_L = \begin{pmatrix} \nu_L \\ \ell_L \end{pmatrix}. \tag{2}$$

Expanding the SU(2) components yields

$$-\lambda_d^{ij} \bar{d}_{\alpha R}^i (V_\alpha e_L^j - Y_\alpha \nu_L^j) + \text{H.c.} \tag{3}$$

In addition to the LQ, we introduce a dark sector with a scalar S and a fermion χ, with a Z_2 symmetry under which the dark sector is odd, whereas the SM and LQ sector is even. Thus, our new physics content is

$$\tilde{R}_2 = (3, 2, 1/6)_+$$

$$S = (1, 3, 0)_- = \begin{pmatrix} \frac{1}{\sqrt{2}} S^0 & S^+ \\ S^- & -\frac{1}{\sqrt{2}} S^0 \end{pmatrix}, \tag{4}$$

$$\chi = (1, 1, 0)_-, \tag{5}$$

where we have also displayed the Z_2 quantum numbers as a subscript. Notice that there is almost no freedom in choosing the above particle content. The quantum charges of the dark sector are fixed by symmetries; either the scalar S or the fermion χ has to be a triplet under $SU(2)_L$ (having both singlets will not give enough charged leptons in the final state to match the CMS study, as we will see). We have chosen a scalar triplet for convenience; the discussion and results would be analogous for a model with a triplet fermion χ and a singlet scalar S. The hypercharge of the dark sector is fixed to be zero to easily accommodate DM direct detection limits.

The LQ decay into the dark sector can then be described by adding the following dimension-five effective operators:

$$-\frac{h_i}{\Lambda_1} S\bar{Q}_i\chi\tilde{R}_2 - \frac{h_i'}{\Lambda_2} S\bar{\ell}_i\chi\tilde{H}, \tag{6}$$

where $\tilde{H}$ is the isospin transformation of the Higgs doublet [13].

The CMS study does not discuss the relative number of e^+e^- and $\mu^+\mu^-$ events in the $\ell^+\ell^- jjE_T$ excess. We will assume them to be equal and introduce both a first generation LQ and a second generation LQ in order to obtain both e^+e^- and $\mu^+\mu^-$ events. In the following, however, we will describe our methods for first generation LQs, keeping in mind that second generation LQs can be similarly treated by a simple replacement of electrons by muons.

III. SPECTRUM AND DECAYS

Either the triplet component S^0 or the singlet χ can be the lightest DM particle. The two possibilities lead to distinct DM phenomenology. Here, we will mainly consider the case of a singlet χ as the DM candidate.

The two couplings of the LQ induce two decay modes: $\tilde{R}_2 \to ej$ and $\tilde{R}_2 \to Sj\chi$. The latter coupling in Eq. (6) induces the $S \to e\chi$ and $S \to \nu\chi$ decays of S. In components, $S^\pm \to \chi e^\pm$, $S^0 \to \nu\chi$, so that decays of charged scalars $S^\pm$ give charged leptons and $\not{E}_T$ in the final state. One loop electroweak corrections induce a small mass splitting of ≈ 200 MeV between the neutral and charged states in S. Combining all decays, one $\tilde{R}_2$ LQ can produce the following final states:

(1) A charged lepton and a jet. The free couplings of the Lagrangian allow us to set the $\tilde{R}_2$ branching ratio to the level required to be compatible with CMS searches for first and second generation LQs, with final states $eejj$ and $e\nu jj$, and similarly for muons. We will find that at the benchmark point of this study, there is no excess in these channels; thus, we will choose

$$\mathrm{BR}(\tilde{R}_2 \to ej) \sim 0\%,$$

consequently $\mathrm{BR}(\tilde{R}_2 \to Sj\chi) \sim 100\%$.

(2) A jet and missing energy ($\not{E}_T$), with

$$\mathrm{BR}(\tilde{R}_2 \to S^0 j\chi \to j\not{E}_T) \sim 29\%.$$

(3) A charged lepton, a jet and missing energy, with

$$\mathrm{BR}(\tilde{R}_2 \to S^\pm j\chi \to \ell^\pm j\not{E}_T) \sim 71\%.$$

IV. CONSTRAINTS ON THE MASSES OF $\tilde{R}_2$, S, χ

(i) Constraints from $j\not{E}_T$ searches. LQ pairs decaying to jets and missing energy must be compatible with $j\not{E}_T$ searches from ATLAS [18] and CMS [19]. The most relevant exclusion limits from these searches are phrased in the squark-neutralino $(m_{\tilde{q}}, m_{\tilde{\chi}_1^0})$ mass plane (Fig. 10 of [18]), where the lightest neutralino is stable and escapes the detector. In our model, both S^0 and χ escape undetected. To compare to the experimental studies, we map the neutralino mass $m_{\tilde{\chi}_1^0}$ to $m_S + m_\chi$ and the squark mass $m_{\tilde{q}}$ to $m_{\tilde{R}_2}$. Taking into account that, in our case, $\mathrm{BR}(\tilde{R}_2 \to j\not{E}_T) \sim 29\%$, we conservatively estimate the bound

$$m_S + m_\chi > 300 \text{ GeV} \tag{7}$$

for LQs in the mass range 450–650 GeV.

(ii) Constraints from CMS LQ searches: There is mild evidence for $\sim$550–650 GeV first generation scalar LQs, using 19.6 fb^{-1} of integrated luminosity, at 2.4σ and 2.6σ, in the $eejj$ and $e\nu jj$ channels, respectively [14]. A branching $\mathrm{BR}(\tilde{R}_2 \to ej) \sim 15\%$ agrees well with the observed excess in the 550–650 GeV mass range. For second generation LQs,

studies of the $\mu\mu jj$ and $\mu\nu jj$ final states have resulted in the exclusion of scalar LQs with masses below 1070 (785) GeV for $\mathrm{BR}_{\mu j} = 1(0.5)$ [15].

As stated before, we will assume a branching $\mathrm{BR}(\tilde{R}_2 \to ej) \sim 0\%$ to switch off decays to this channel for LQs of mass around 500 GeV. We will also assume $\mathrm{BR}(\tilde{R}_2 \to \mu j) \sim 0\%$ to be compatible with second generation LQ searches.

(iii) Constraints from the dilepton invariant mass $m_{\ell\ell}$ distribution of the CMS $\ell^+\ell^- jj\not{E}_T$ excess, located mostly below $m_{\ell\ell} \approx 80$ GeV. The two leptons in our case come from the decay $S \to \ell\chi$. To get the excess in the required range the mass difference between S and χ should be $m_S - m_\chi \sim 20$–40 GeV spectra where $m_S - m_\chi \gtrsim 40$ GeV is disfavored since the dilepton invariant mass distributions would peak at a value of $m_{\ell\ell}$ that is too large compared to the excess. On the other hand, for $m_S - m_\chi \lesssim 20$ GeV, the leptons are too soft and do not survive the p_T cuts for leptons.

V. RESULTS

We take our background estimates from [1]. Opposite-sign opposite-flavor leptons from $t\bar{t}$, which has the same rate of the same-flavor (OSSF) channel, are used to measure these backgrounds in the CMS study. Drell-Yan (DY) production, the main irreducible background, is estimated by a control region which does not overlap with the signal region.

We follow the CMS counting experiment analysis in [1] for the signal. The final state is required to have at least two leptons and at least two jets. The cuts employed are as follows.

Cut (i): Two OSSF leptons are required to be present, with $p_T > 20$ GeV in $|\eta| < 1.4$, which is defined as the *central region* in the CMS study.

Cut (ii): At least two jets are required with $p_T > 40$ GeV in $|\eta| < 3.0$.

We use FASTJET [20] to reconstruct the jets. An event is selected if it contains two jets and satisfies $\not{E}_T > 150$ GeV, or if it contains three or more jets and satisfies $\not{E}_T > 100$ GeV. In the dilepton invariant mass range 20 GeV $< m_{\ell\ell} < 70$ GeV, the total background estimate provided by the CMS study for central OSSF events is 730 ± 40. The observed number was 860, corresponding to an excess of 130^{+48}_{-49} events provided by new physics, we hypothesize. In our model, this excess number of events is produced by first and second generation LQs. We implement the model in FEYNRULES [21] and calculate the branching ratios and cross sections using MADGRAPH [22]. The events are then passed onto PYTHIA [23] for parton showering and hadronization followed by the modeling of detector effects by DELPHES [24]. We took exactly the same electron/muon/jets isolation criteria adopted in [1]. Production cross sections were normalized

TABLE I.   Summary of the effective cross sections (fb) for some benchmark signal points that best fit the CMS signal at LHC8. In the fourth and fifth rows of each point we also show in parenthesis the final number of events predicted. The last row displays the number of events in the forward region. Masses are in GeV. Lagrangian parameters are fixed at $\lambda_d^{ij} = 10^{-4}$, $h_i/\Lambda_1 = 10^{-3}$ GeV^{-1} and $h_i'/\Lambda_2 = 10^{-3}$ GeV^{-1}. The benchmark point for the current study is C. The cross sections (in fb) predicted at LHC14 after imposing the cuts of the LHC8 analysis for the three best benchmark points are displayed in the last column.

$(m_{\tilde{R}_2}, m_S, m_\chi)$	Selection	Signal (fb)	Signal$_{14}$ (fb)
	Preselection	149.1	
$A: (450, 200, 170)$	Cut (i)	40.2	46.6
	Cut (ii)	10.5	
	$20 < m_{\ell\ell} < 70$	5.7(110)	
	$m_{\ell\ell} > 100$	1.8(37)	
	Forward	18	
	Preselection	105.7	
$B: (500, 200, 170)$	Cut (i)	28.5	69.6
	Cut (ii)	11.6	
	$20 < m_{\ell\ell} < 70$	5.7(112)	
	$m_{\ell\ell} > 100$	2.3(45)	
	Forward	14	
	Preselection	126.1	
$C: (500, 160, 140)$	Cut (i)	19.0	53.6
	Cut (ii)	10.0	
	$20 < m_{\ell\ell} < 70$	5.8(114)	
	$m_{\ell\ell} > 100$	1.11(21)	
	Forward	8	

by the next-to-leading-order (NLO) QCD rate using PROSPINO2.1 [25].

We performed a scan over the masses $(m_{\tilde{R}_2}, m_S, m_\chi)$, fixing the Lagrangian parameters $\lambda_d^{ij} = 10^{-4}$, $h_i/\Lambda_1 = 10^{-3}$ GeV^{-1} and $h_i'/\Lambda_2 = 10^{-3}$ GeV^{-1}. In the above, we have assumed democratic values for the Yukawas corresponding to $i = 1, 2$ and $j = 1, 2$. We note that constraints arising from meson decays and mixings are sensitive to products of the Yukawas λ^{ij}; in particular, our choice of Yukawas is compatible with bounds given in [26] and [13]. The cut flow is displayed in Table I for some spectra that best fit the number of events in the central region of the CMS search with BR($\tilde{R}_2 \to ej$) $\sim 0\%$, $m_S + m_\chi > 300$ GeV and $m_S - m_\chi < 40$ GeV.

We have assumed theoretical uncertainties following [27] which are the same as the estimates used by CMS in its LQ search [1]. The uncertainties are given in Table 1 of the CMS paper [1]. Variation of the renormalization/ factorization scale between half and twice the LQ mass leads to a $\sim 25\%$ uncertainty in the production cross section. The parton distribution function uncertainty is approximately 20% of the NLO cross section. This can easily lead to a $\sim 20\%$ variation in the number of signal events, which will be interesting to pursue if the signal becomes stronger in the next run.

In Fig. 1, we show the comparison between the CMS data points and the predicted distribution for our model at benchmark point C. As we see, our model can fit the data very well. In fact, points A, B and C of Table I present this feature. While the CMS study showed a triangular shape with a sharp edge, for benchmark point C around 21 events survive in the region $m_{\ell\ell} > 100$ GeV, which is well within the background uncertainty.

In order to better quantify the agreement between these model predictions and the data we used the χ^2 statistics defined below in Eq. (8), which, as in the experimental study, compares a model prediction in the central ($|\eta_\ell| < 1.4$) and forward ($1.6 < |\eta_\ell| < 2.4$) regions:

$$\chi^2(\mu) = \min_{\{\theta\}} \sum_{i=1}^{N_{\text{bin}}} \left[\frac{(\mu s_i^I + \theta \cdot \mathbf{b^I}_i - d_i^I)^2}{(\sigma_i^I)^2} + \frac{(\mu s_i^O + \theta \cdot \mathbf{b^O}_i - d_i^O)^2}{(\sigma_i^O)^2} \right]. \quad (8)$$

In this formula, $s_i^{I(O)}$, $\mathbf{b^{I(O)}}_i$ and $d_i^{I(O)}$ denote the ith dilepton invariant mass bin for the signal, backgrounds [DY and flavor-symmetric (FS)] and data distributions, respectively, in the central region. The superscipts I and O denote the inside the window region $20 < m_{\ell\ell} < 70$ GeV and the outside region $m_{\ell\ell} > 70$ GeV, respectively. The corresponding experimental uncertainties in each bin are given by σ_i^I, σ_i^O and σ^F. In order to better approach the uncertainties in the background bins we take into account two nuisance parameters $\theta = (\theta_1, \theta_2)$ for the DY background normalization, b_1, and the FS background normalization b_2.

All these regions are crucial to determine the pattern of decays and the spectra favored by the data. For example, those spectra where the $m_S - m_\chi$ are bigger than ~ 40 GeV are disfavored in this respect as their dilepton invariant mass distributions peak outside the window. On the other hand, for $m_S - m_\chi \lesssim 20$ GeV, the leptons are too soft and do not survive the p_T cuts for leptons. We show in Fig. 2 the dilepton invariant mass distribution for the point C. The CMS study compared their data against a R-parity conserving supersymmetric scenario where an sbottom decays to a SF lepton pair and missing energy. This type of decay presents a dilepton mass distribution with a triangular shape and a kinematic edge around $m_{\tilde{b}} - m_{\chi_2^0}$, which fits the observed excesses well.

The forward region is an important control region since it is expected that heavy particles undergoing decays as in SUSY or LQ models (as suggested in this work) will produce central leptons. We checked that the number of events is small for the best LQ models, around seven events for benchmark C and similarly for the others as shown in Table I. This is consistent with the CMS reported number of 6 ± 20 events in the forward region. Moreover, the expected fraction of signal events with three or more leptons in those
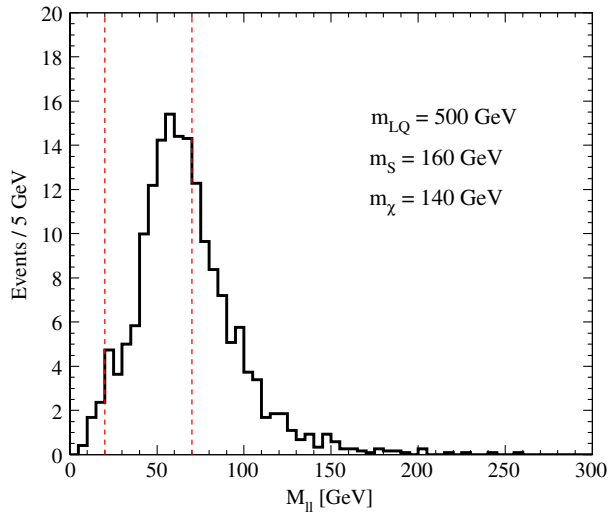
FIG. 2 (color online). The dilepton invariant mass distribution of the signal events (point C) is displayed. The vertical dashed lines indicate the invariant mass cut. Around 21 events survive in the region $m_{\ell\ell} > 100$ GeV, which is well within the background uncertainty.

benchmark points is never beyond 0.5%, again consistent with the absence of an excess in the trilepton channel.

We show in Table II the χ^2 obtained with Eq. (8) and the corresponding p value calculated as $p = \int_{\chi_C^2}^{\infty} \chi_{n-1}^2(x)dx$, where $n = 60$ degrees of freedom, for the LQ models, the SUSY model of the experimental study and the pure background model. The numbers in parenthesis represent the one-sided probability in the tail of a normal distribution. The CMS study assigns a 2.4σ significance for the SUSY model against 2.6σ from our estimate. The discrepancy might be due to the estimation of the errors included in the fit which are not fully accessible to us. Nevertheless, we also found that the best fit is provided by a SUSY-type signal and point B. The benchmark points A, B and C, by their turn, are the best fitting points in our model, as can been seen in Table II, and very similar to the SUSY fit.

With the current data, none of these models can be excluded at 90% C.L., for example, although some models can provide a better fit than others. The background model

TABLE II. The χ^2 statistics computed from Eq. (8) for three benchmark LQ models, the SUSY model and the background model taken from the CMS analysis [1]. In the third column we show the p value of each model and the corresponding statistical significance in parenthesis as described in the text.

Model	χ^2	p value
A	35.0	$0.005(2.5\sigma)$
B	34.3	$0.004(2.6\sigma)$
C	35.0	$0.005(2.5\sigma)$
SUSY	34.3	$0.004(2.6\sigma)$
Background	40.6	$0.03(1.8\sigma)$

is currently the worst fit amongst all of them. Comparing the LQ and supersymmetry interpretations we see that the SUSY model is able to explain the data as well as our best point, B. The benchmark point C, however, is the one that better fits the excess quoted in the CMS work in the signal region $20 < m_{\ell\ell} < 70$ GeV, 114 events against 130 of the CMS fit. Moreover, it predicts the smallest number of events in the forward region of all benchmark points, eight events against six from CMS.

In the last column of Table I we show the projected cross sections at the LHC14 surviving the cuts of the LHC8 analysis for the three best benchmark points found.

VI. COMMENTS ON DARK MATTER PHENOMENOLOGY

DM stability is guaranteed by the discrete Z_2 symmetry. The options are to have either triplet or singlet DM that could be the fermion χ or the scalar S as discussed thoroughly in [13]. Taking into account direct, indirect and collider constraints the following possibilities emerge:

(1) A scalar singlet S coupled to the Higgs portal. After taking LUX, indirect detection and Higgs invisible decay widths into account the mass range $m_S > 100$ GeV and $m_S \sim 60$–65 GeV is allowed. However, XENON1T is expected to masses up to a 1 TeV [28].

(2) A fermionic singlet (χ) with a significant pseudo-scalar coupling to the Higgs portal results in a less constrained spin-dependent scattering cross section [29]. With Λ being the scale of the portal interaction, and $\sin\xi$ the pseudoscalar coupling, from Fig. 7 of [29], it is clear that $m_\chi \gtrsim \mathcal{O}(100)$ GeV is allowed by data for $\sin^2\xi \gtrsim 0.7$ with $\Lambda \sim 1$–5 TeV. The bounds do not depend much on whether χ is Majorana or Dirac.

Thus, a singlet fermionic DM candidate with mass $m_\chi \sim 140$ GeV that we have taken in our collider analysis of this paper is currently a viable option.

VII. CONCLUSIONS

In this paper, we have shown that the excess observed by CMS in the $\ell^+\ell^- jj\not{E}_T$ search can be explained consistently within a class of LQ models. We particularly discussed a model which consists of scalar first generation and second generation LQs that decay dominantly to leptons, jets and missing energy in the form of a stable DM candidate. The confluence of proton decay constraints and DM direct/indirect detection results in a highly predictive model of LQs that can satisfy the CMS $\ell^+\ell^- jj\not{E}_T$ search. Our model provides a general proof of concept that a peak distribution in the required dilepton mass range can be obtained outside the purview of supersymmetry.

Benchmark point C consists of first and second generation LQs with masses of 500 GeV, and dark sector particle masses of $m_S = 160$ GeV and $m_\chi = 140$ GeV.

The LQs dominantly decay to $\ell j \not{E}_T$ final states ($\sim$71% branching), and subdominantly into $j \not{E}_T$ final states ($\sim$29% branching), while there is negligible branching into the canonical LQ final states of ℓj.

While CMS fit a triangular shape in the opposite-sign same-flavor dilepton invariant mass distribution after event selection and flavor subtraction, it is too premature to settle definitively on a kinematic edge. In our model, the number of signal events in the window $20 < m_{\ell\ell} < 70$ GeV after event selection is 114 for the benchmark point. The dilepton mass distribution peaks in the window between 20–70 GeV with the required event count, while the number of events in the region $m_{\ell\ell} > 100$ GeV is within the background uncertainty. In a simple χ^2 fit, this point compares favorably with the CMS SUSY fit in [1]. The model is consistent with the nonobservation of a signal in the forward region, and in the trilepton final states. We have also provided projections for the signal cross sections at LHC14 in the best benchmark models. For the benchmark point C, for example, $\sim$5360 events are expected with 100 fb^{-1} luminosity.

These results highlight the importance of refining the search strategy and that a potential LQ discovery is attainable in the next LHC run.

[1] CMS Collaboration, Report No. CMS-PAS-SUS-12-019, 2014.

[2] B. Dutta, T. Kamon, N. Kolev, K. Sinha, K. Wang, and S. Wu, Top squark searches using dilepton invariant mass distributions and bino-Higgsino dark matter at the LHC, Phys. Rev. D **87**, 095007 (2013).

[3] B. Allanach, A. R. Raklev, and A. Kvellestad, Interpreting a CMS $lljjp_T^{\mathrm{miss}}$ excess with the golden cascade of the MSSM, Phys. Rev. D **91**, 115022 (2015).

[4] P. Huang and C. E. M. Wagner, CMS kinematic edge from sbottoms, Phys. Rev. D **91**, 015014 (2015).

[5] P. Grothaus, S. P. Liew, and K. Sakurai, A closer look at a hint of SUSY at the 8 TeV LHC, J. High Energy Phys. 05 (2015) 133.

[6] J. C. Pati and A. Salam, Lepton number as the fourth color, Phys. Rev. D **10**, 275 (1974); **11**, 703(E) (1975).

[7] H. Georgi and S. L. Glashow, Unity of All Elementary Particle Forces, Phys. Rev. Lett. **32**, 438 (1974).

[8] E. Farhi and L. Susskind, Technicolor, Phys. Rep. **74**, 277 (1981); S. Dimopoulos and L. Susskind, Mass without scalars, Nucl. Phys. **B155**, 237 (1979).

[9] J. L. Hewett and T. G. Rizzo, Much ado about leptoquarks: A comprehensive analysis, Phys. Rev. D **56**, 5709 (1997).

[10] M. Leurer, A comprehensive study of leptoquark bounds, Phys. Rev. D **49**, 333 (1994).

[11] S. Davidson, D. C. Bailey, and B. A. Campbell, Model independent constraints on leptoquarks from rare processes, Z. Phys. C **61**, 613 (1994).

[12] S. S. Gershtein, A. A. Likhoded, and A. I. Onishchenko, TeV-scale leptoquarks from GUTs/string/M-theory unification, Phys. Rep. **320**, 159 (1999); I. Dorsner and P. Fileviez Perez, Unification without supersymmetry: Neutrino mass, proton decay and light leptoquarks, Nucl. Phys. **B723**, 53 (2005); B. Gripaios, Composite leptoquarks at the LHC, J. High Energy Phys. 02 (2010) 045; P. Fileviez Perez, T. Han, T. Li, and M. J. Ramsey-Musolf, Leptoquarks and neutrino masses at the LHC, Nucl. Phys. **B819**, 139 (2009); P. Y. Popov, A. V. Povarov, and A. D. Smirnov, Fermionic decays of scalar leptoquarks and scalar gluons in the minimal four color symmetry model, Mod. Phys. Lett. A **20**, 3003 (2005); K. S. Babu and J. Julio, Two-loop neutrino mass generation through leptoquarks, Nucl. Phys. **B841**, 130 (2010).

[13] F. S. Queiroz, K. Sinha, and A. Strumia, Leptoquarks, dark matter, and anomalous LHC events, Phys. Rev. D **91**, 035006 (2015).

[14] CMS Collaboration, Report No. CMS-PAS-EXO-12-041, 2014.

[15] CMS Collaboration, Report No. CMS-PAS-EXO-12-042, 2012;ATLAS Collaboration, Search for second generation scalar leptoquarks in pp collisions at $\sqrt{s} = 7$ TeV with the ATLAS detector, Eur. Phys. J. C **72**, 2151 (2012); Search for pair production of third-generation scalar leptoquarks and top squarks in proton-proton collisions at $\sqrt{s} = 8$ **TeV**, Phys. Lett. B **739**, 229 (2014); Report No. CMS-PAS-EXO-13-010, 2014.

[16] W. Buchmuller, R. Ruckl, and D. Wyler, Leptoquarks in lepton-quark collisions, Phys. Lett. B **191**, 442 (1987); **448**, 320(E) (1999).

[17] A. J. Davies and X. G. He, Tree level scalar fermion interactions consistent with the symmetries of the standard model, Phys. Rev. D **43**, 225 (1991).

[18] ATLAS Collaboration, Search for squarks and gluinos with the ATLAS detector in final states with jets and missing transverse momentum using $\sqrt{s} = 8$ TeV proton-proton collision data, J. High Energy Phys. 09 (2014) 176.

[19] CMS Collaboration, Search for new physics in the multijet and missing transverse momentum final state in proton-proton collisions at $\sqrt{s} = 8$ TeV, J. High Energy Phys. 06 (2014) 055.

[20] M. Cacciari, G. P. Salam, and G. Soyez, FASTJET user manual, Eur. Phys. J. C **72**, 1896 (2012).

[21] N. D. Christensen and C. Duhr, FEYNRULES—Feynman rules made easy, Comput. Phys. Commun. **180**, 1614 (2009).

[22] J. Alwall, M. Herquet, F. Maltoni, O. Mattelaer, and T. Stelzer, MADGRAPH 5: Going beyond, J. High Energy Phys. 06 (2011) 128.

[23] T. Sjostrand, S. Mrenna, and P. Z. Skands, PYTHIA 6.4 physics and manual, J. High Energy Phys. 05 (2006) 026.

[24] J. de Favereau, C. Delaere, P. Demin, A. Giammanco, V. Lemaître, A. Mertens, M. SelvaggiDELPHES 3 Collaboration, DELPHES 3, A modular framework for fast simulation of a generic collider experiment, J. High Energy Phys. 02 (2014) 057.

[25] W. Beenakker, R. Hopker, and M. Spira, PROSPINO: A program for the production of supersymmetric particles in next-to-leading order QCD, arXiv:hep-ph/9611232.

[26] I. Dorsner, S. Fajfer, and A. Greljo, Cornering scalar leptoquarks at LHC, J. High Energy Phys. 10 (2014) 154.

[27] M. Kramer, T. Plehn, M. Spira, and P. M. Zerwas, Pair production of scalar leptoquarks at the CERN LHC, Phys. Rev. D **71**, 057503 (2005).

[28] F. S. Queiroz and K. Sinha, The poker face of the Majoron dark matter model: LUX to keV line, Phys. Lett. B **735**, 69 (2014); J. M. Cline, K. Kainulainen, P. Scott, and C. Weniger, Update on scalar singlet dark matter, Phys. Rev. D **88**, 055025 (2013); L. Feng, S. Profumo, and L. Ubaldi, Closing in on singlet scalar dark matter: LUX, invisible Higgs decays and gamma-ray lines, J. High Energy Phys. 03 (2015) 045; C. Kouvaris, I. M. Shoemaker, and K. Tuominen, Self-interacting dark matter through the Higgs portal, Phys. Rev. D **91**, 043519 (2015).

[29] M. A. Fedderke, J. Y. Chen, E. W. Kolb, and L. T. Wang, The fermionic dark matter Higgs portal: An effective field theory approach, J. High Energy Phys. 08 (2014) 122.